J. Basic. Appl. Sci. Res., 3(2s)443-452, 2013

ISSN 2090-4304
Journal of Basic and Applied Scientific Research
www.textroad.com

Occurrence of Induction Earthquakes in the Caspian Region

Mohammad Reza Ebrahimi, Ali Amjadi, Shamsedin Esmaeili, Hosein Nesari

Department of Civil Engineering, Eyvan-e-Gharb Branch, Islamic Azad University, Eyvan, Iran

Received: June 10 2013
Accepted: July 10 2013

ABSRACT

Caspian zone seismotectonics of the Iranian plateau, one of the world's most active seismotectonic zones are located. Observations and studies have shown that excessive accumulation of water on the dam in the past few years has been significant seismicity. Our regional seismicity using fractal dimension of space, and it changes the pattern of aftershocks and earthquakes and aftershocks in the region, we compared the relationship deteriorated. About 1943 earthquakes in the period 1902/02/13 to 2009/09/21 were used for the calculation. The study region includes 1943 earthquakes that was divided into $0.3^0 \times 0.3^0$ networks and put on an overlap about 15^0 to display a more comprehensive picture of the fractal distribution. Fractal dimension (D) of earthquakes in each grid was calculated results show a good correlation between D and the pattern of earthquakes and aftershocks of earthquakes and aftershocks induced decline of the relationship, which represents the earthquake their induction into the Caspian.
KEYWORDS: fractal dimension, the earthquake and aftershocks, Caspian, seismic induced.

1. INTRODUCTION TO DATA

To study the effect of weight on seismic Caspian region and the induction of some earthquakes occurred in the region in the first step, the earthquake occurred at 45 to 56 ° East longitude and latitude 35-48° North Geophysics Institute of Tehran University Seismic Network catalog and catalogs of the International Institute of Seismology and Earthquake Engineering, was obtained (Figure 1). A total of 19465 earthquakes in the period 1902/02/13 to 2009/09/21 was extracted from the Catalog**.** In order to carry out more detailed studies on the possibility of induced earthquake zone**,** Since the epicenter of the earthquake mostly on the lower part of the lake and its surrounding lakes are very close distances**,** So earthquakes along the lake margins outside the box shown in Figure (1) is known, was excluded**.** Number of events remaining after the removal of the 1943 earthquake earthquakes decreased (Fig. 2) and statistical analysis to detect induction of seismic data was carried on.

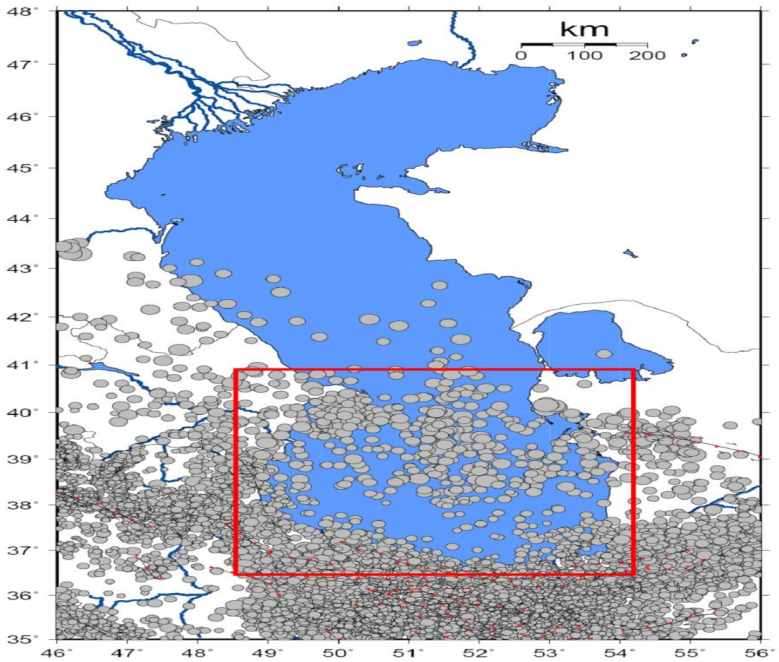

Figure 1: Total 19465 earthquakes Geophysics Institute of Tehran University Publications Catalog Seismic Network

***Corresponding Author:** Ali Amjadi, Department of Civil Engineering, Eyvan-e-Gharb Branch, Islamic Azad University, Eyvan, Iran. Email address: Amjadi_gp@yahoo.com@yahoo.com

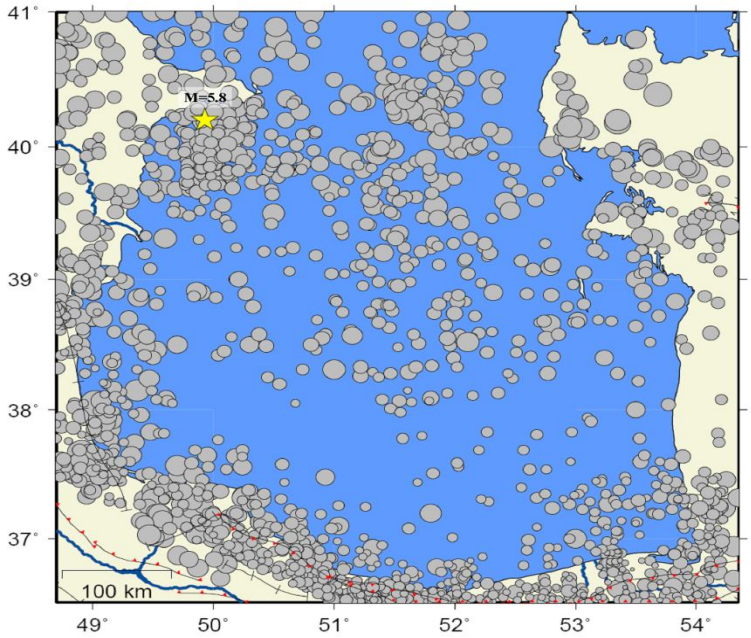

Figure 2 : earthquakes located in the lower part of the lateral margin of the lake, the location of earthquakes with magnitude 5.8 stars is shown in Fig.

2. METHOD OF DETECTION

2.1 Investigating the pattern of earthquakes and aftershocks

The pattern of earthquakes and aftershocks can be divided into three categories, as shown in (figure 3) can be classified (Mogi, 1963).

The difference between this three models and the spatial distribution of stresses in the material structure is as follows:

Type 1 - In the case of homogeneous materials and stress effects are the same, no major earthquakes have occurred before the earthquake and many aftershocks is associated with elastic.

Type 2 - When the materials are relatively homogenous structure and applied stresses are not uniform, elastic principal earthquakes occurring small earthquakes before and after large aftershocks will occur.

Type 3 - in the case of highly heterogeneous structure, material, or focus on specific areas of applied stress and not uniform, Magnitude of the earthquake at first increases and then decreases over time.

But the aftershocks of the earthquake patterns in Mogi type 2 pattern of induced earthquakes are followed, the frequency of earthquakes and earthquake rises, And then we will see a decline in the aftershocks, earthquakes that while they follow the normal pattern of type 1.

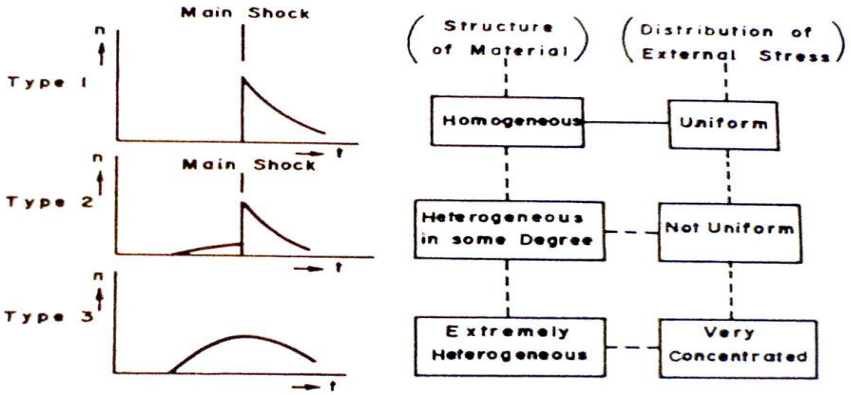

Figure 3: the pattern of earthquakes and aftershocks and their relationship with the structure of materials and stress (Moogi, 1963)

Figure (4 - a) the total number of earthquakes occurred from 13/02/1902 to 21/09/2009 on an annual basis is shown. It is observed that the frequency of earthquakes is very low in 1986, Hence the frequency of the event for more scrutiny after the 1986 earthquake in Figure (4 - b) is shown. As of the form (4 - b) implies a large increase in the frequency of earthquakes in the late 2000 is seen as a way of Mogi model of type 2 follows. In order to further investigate the occurrence of earthquakes, Earthquakes within a month from the time the fish that we saw a sharp increase in earthquakes Separated from

the remaining data and the total number of earthquakes occurring on a daily basis according to the one-month period (5) were plotted. As can be seen in this figure, as well as seeing an increasing trend for the occurrence of aftershocks of a large earthquake, a magnitude 8/5 on 25/11/2000're in position, Figure (2) marked with an asterisk and then we see a decreasing trend for aftershocks, so you can see exactly this pattern for earthquakes induced type 2 Mogi agrees.

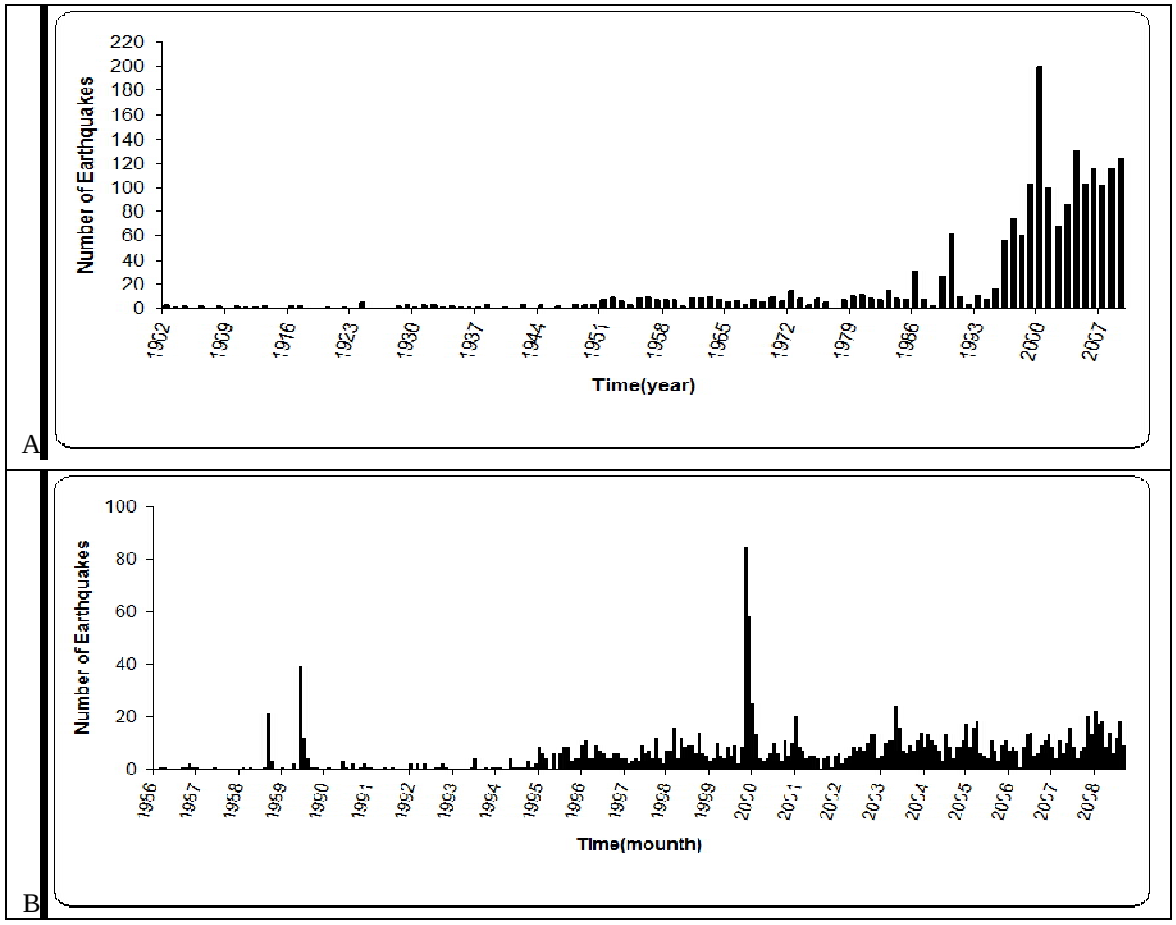

Figure 4: (a) earthquake occurred from 13/02/1902 to 21/09/2009 on an annual basis
(B): earthquakes occurred from 01/01/1986 to 21/09/2009 on a monthly basis

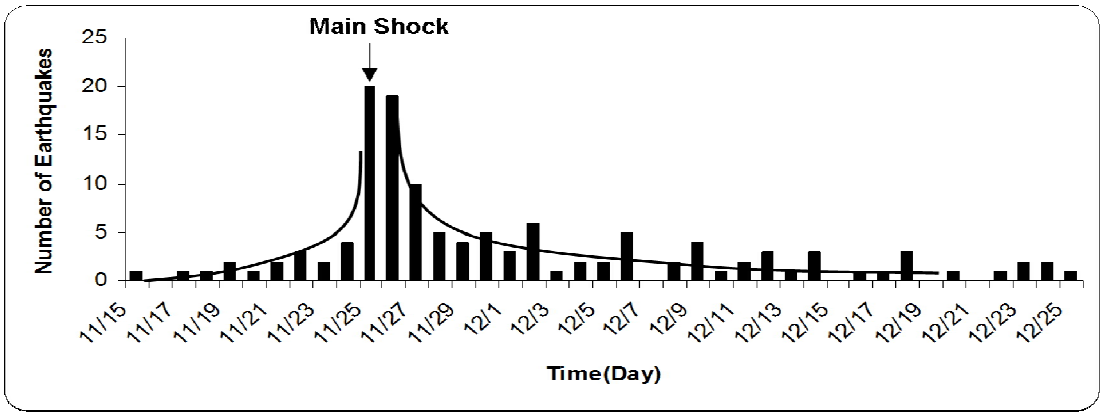

Figure 5: the pattern of earthquakes and aftershocks of the great earthquakes 25/11/2000 , M=5.8 on a daily basis

2.2 Considering the decay of aftershocks

Based on Utsu (1961) Distribution of aftershocks in time can be expressed by the following equation:

$$n(t) = ct^{-h} \quad (1)$$

Where $n(t)$ m is the frequency of aftershocks per unit time, and the coefficients are constant and the time elapsed after the main earthquake. Coefficient indicating the rate of decline in the frequency of aftershocks and can it be used to influence the location and physical stress conditions (Mogi, 1962). Based on Utsu studies, the initial curve in reasonable

frequency of aftershocks of up to 100 days from the above equation follows. After this time, the following equation can be used:

$$n(t) = c_1 e^{-pt} \qquad (2)$$

Where c_1 and p are constant coefficients. However, Noor and Booker (1972) found that the earthquake of 1966, Parkfield - Choulam one of the best records are the earthquakes, The frequency of aftershocks in the relations between $t^{-1/2}$ and $t^{-3/4}$ times longer than the relationship that follows t^{-1}. Gupta et al (1972) found that the values of h for dehydration due to induced earthquakes are smaller than natural earthquakes. In recent decades, attenuation of induced earthquakes aftershocks many examined and it is clear that the natural attenuation of ground motion with speeds less. Table (1) by Gupta and Rastogi (1976) has been prepared in which the aftershocks of earthquakes induced deterioration of relations are different.

Table 1: relationships presented for the decay of aftershocks (Gupta and Rastogi, 1976)

Region	$n(t) = Ct^{-h}$	Unit of time	Total time
Kariba	$130t^{-1.0}$	1 day	60 days
Kremasta	$134t^{-0.78}$	1 day	200 days
Koyna	$180t^{-1.0}$	1 day	110 days
Koyna	$1{,}342t^{-0.77}$	15 days	Dec. 1967 to Dec. 1971
Kurobe	$Ct^{-0.67}$	cumulative	Nov. 16, 1968 to April 1970
Hsinfengkiang	$Ct^{-0.90}$	cumulative	96 days
Oroville	$Ct^{-0.70}$	hours	10 days
Oroville	$112t^{-0.78}$	1 day	100 days
Aswan	$20t^{-1.0}$	1 day	100 days
Bhatsa	$300t^{-1.0}$	1 day	500 days

To calculate the decay rate of aftershocks in the region because of the aftershocks at intervals of less than 100 days, the equation (1) is provided by Utsu was used.
The result obtained by this selection acts on the aftershocks of the earthquake in Table (2) is observed. How to apply this equation to the data in Figure (6) is on display.

Table 2: The relationship obtained for the decay of aftershocks activity

Date of occurrence	$n(t) = ct^{-h}$	Time units	Total time
2000/11/25	$n(t) = 20t^{-1.052}$	1 days	31 days

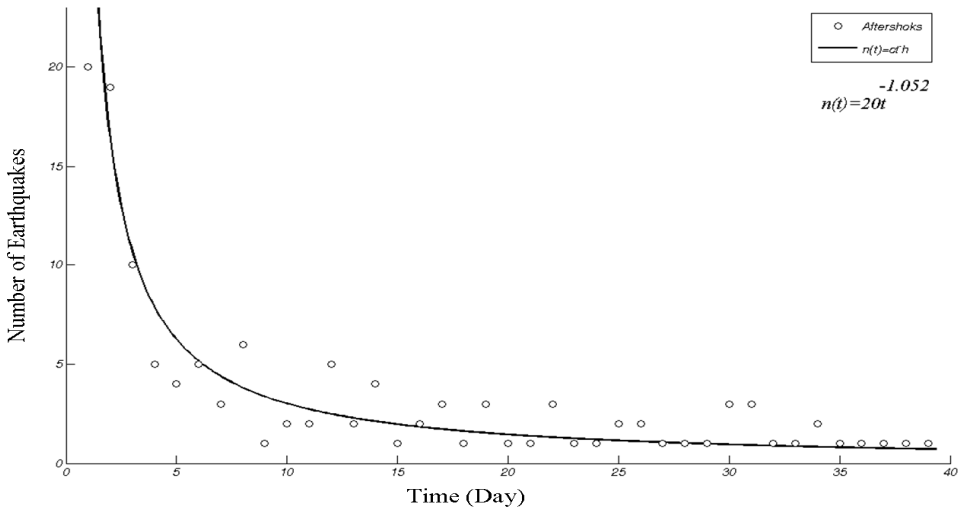

Figure 6: deterioration of the relationship for aftershocks with magnitude quake 25/11/2000 M=5.8 on a daily basis

h values due to earthquake induced flooding is smaller than natural earthquakes (h <1) and the values of the ratio of early (h ≈0.75)$t^{-\frac{3}{4}}$ is reduced. And the days are longer during the main earthquake tend to (h = 1)t^{-1}, for earthquake Elected as shown in Table (2) can be seen amount of 1/052h is obtained for total time 31 days. As can be seen the h ratio is about 1, the results for selected events with the results presented in Table (1) for different samples of induced earthquakes are a good match.

2-3 Considering the fractal distribution of earthquakes

Earthquakes occur on faults and fault activation, in turn, can result in fractured rock, and hence, earthquakes can be represented by a structure similar to mathematics (Chandrani Singh et al, 2008). Fractal parameters such that the resulting structure is called self-similar fractal dimension is defined. Fractal dimension as a complex statistical tools to determine the subsequent distribution of earthquakes, how they happen to be randomized as well as spatial categories are used to earthquakes (Knopoff, Kagan 1980 and, Hirata, 1989). Various processes such as batch processes and continuous displacement on faults such as folds are very complex, but they follow fractal mathematics (Mandelbrot, 1982)**.** Various processes such as batch processes and continuous displacement on faults such as folds are very complex, but they follow fractal mathematics (Mandelbrot, 1982)**.** Fractal geometry of faults in different aspects of the world has been estimated by many researchers (San Andreas Fault by Aviles et al, 1987; Okubo and Aki, 1987, in Japan Shimazaki and Nagahama, 1995 in India Bhattacharya et al, 2002). Their studies showed that D values are in the range of 0 to 3. D value close to 3 indicate that seismic fractures in a volume of the crust are**,** A value close to 2, indicating a level of exposure, and a value close to 1 means the springs linearity is mainly**.** (Aki, 1981) and Tosi (1988) proposed that the fractal dimension of earthquakes are confined between 0 to 2 that dependent to Space covered by a fractal object. $D \to 0$ Is the set of all events are concentrated at one point and $D \to 2$ is the sense of random events or are distributed uniformly on a two-dimensional space. Shimazaki and Nagahama (1995) showed that the active fault systems in Japan are self-similar structure with fractal dimension of 5/0 to 6/1. Aviles and his colleagues (1987) also showed that the amount of D in different parts of the San Andreas Fault from 1/8000 to 1/1910 is changed.

On the relationship between fractal dimensions D seismic has done extensive research over the past three decades (Aki, 1981; King, 1983; Turcotte, 1986; Hirata, 1989, Wang, 1991; Volant and Grasso, 1994; Oncel and et al, 1996, Lapenna et al, 1998; Henderson et al, 1999; Legrand, 2002; Wyss et al, 2004; Mandal and Rastogi, 2005). These studies show that the fractal dimension D of the normative change is consistent with the earthquakes. For example, the rule changes have already occurred coefficient D has had a major quake (Jan Robys et al, 1993; Legrand et al, 1996). Research results Chandrani Singh and his colleagues (2008) demonstrated that, in areas where earthquakes occur induction coefficient D is generally small and less than one. The most common methods for determining the fractal dimension are two ways (Grassberger and Procaccia, 1983):

1) Count the number of events in each square of the grid area (Box counting) that in this way the valence (oD) is calculated.

2) The correlation (Correlation dimension).

In the first method, an active fault system is divided by the square lattice. In this way, the grid can be used with different dimensions. But this method is not reliable enough, especially when there is limited data (Hirata, 1989). Hence, we do not use this technique in studies of correlation integral Box counting method is preferred, It is much more reliable and more sensitive to small changes in the properties of the spatial clustering of earthquakes is (Hirata, 1989). The correlation is given as follows (Grassberger and Procaccia, 1983)

$$D_{wr} = \lim \log(C_r)/\log r \qquad r \to 0 \tag{3}$$

Where C_r is correlation function that spatial sorting between a set of points to be measured, and is presented as follows:

$$C(r) = \frac{2}{N(N-1)} N(R < r) \tag{4}$$

Where N (R <r), the number of pairs (X_i, Xj) the separation is smaller than r. Integral correlation is related to the standard correlation function is defined as follows:

$$\mathrm{C}(\mathrm{r}) \sim \mathrm{rD}_2 \tag{5}$$

Where D_2 is the fractal dimension or correlation dimension (Grassberger and Procaccia, 1983), and of D, then we call it.

Distance (r) between two events $(\theta_1, \phi_1), (\theta_2, \phi_2)$ related by a Spherical Trigonometry by Hirata (1989) is:

$$r = \cos^{-1}[\cos\theta_1 \cos\theta_2 + \sin\theta_1 \sin\theta_2 \cos(\phi_1 - \phi_2)] \tag{6}$$

Where θ_1, θ_2 geographical longitudes and ϕ_1, ϕ_2 are geographical latitudes during events 1 and 2.

D coefficient of the logarithmic-logarithmic diagram slope by fitting to a line is obtained using least squares method (Fig. 7).

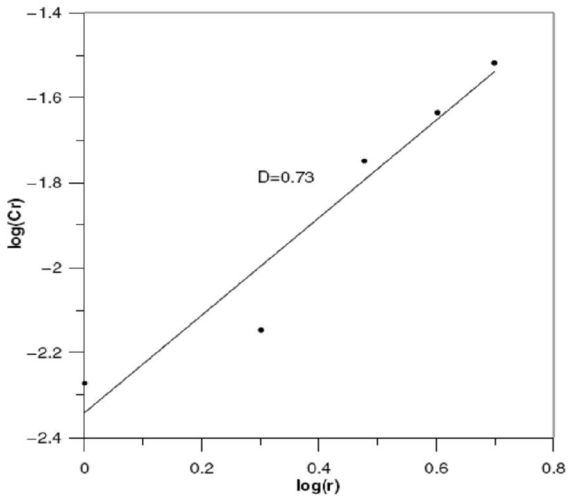

Figure 7: Example of D estimated from the correlation integral.
Logarithmic Chart - log of C (r) and r.

To showing fractal spatial dimension, the study area includes 1943 earthquakes are classified into $0.3^0 \times 0.3^0$ grid, and an overlap of 0.15^0 for a more comprehensive view of the distributed fractal image set was applied (Fig. 8). by doing so, the 49 network forms (9, 10) were generated. Networked together to effectively impose on and given the number of networks that are more than 20 events were considered in the calculations. Number of data in the network is varied between 20 to 57 events. Since the error in the epicenter of earthquakes depth error is much smaller than the fractal dimension of earthquakes epicenter was studied.

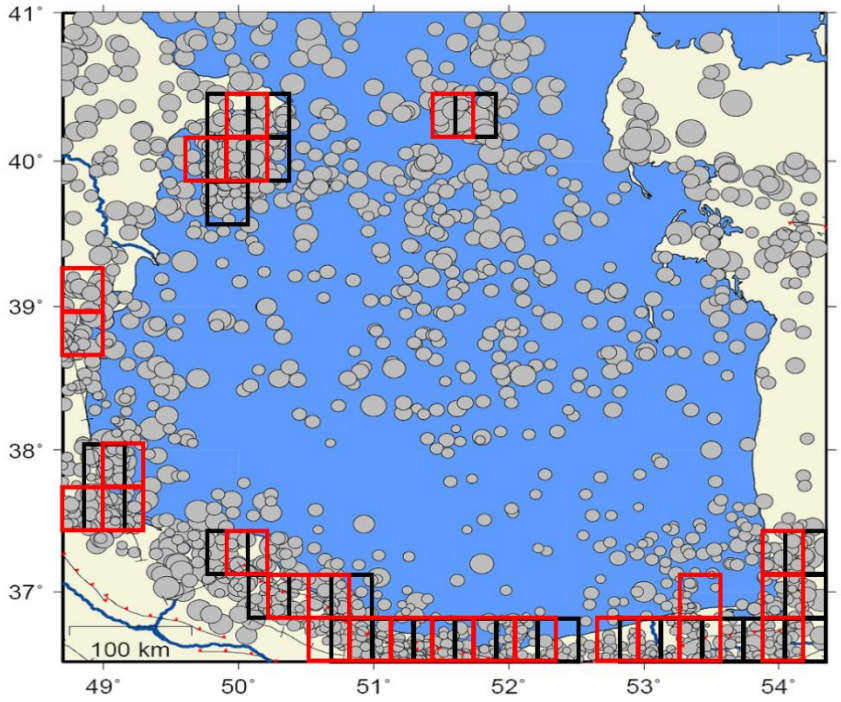

Figure 8: how grid size used in the study area to estimate the spatial fractal dimension

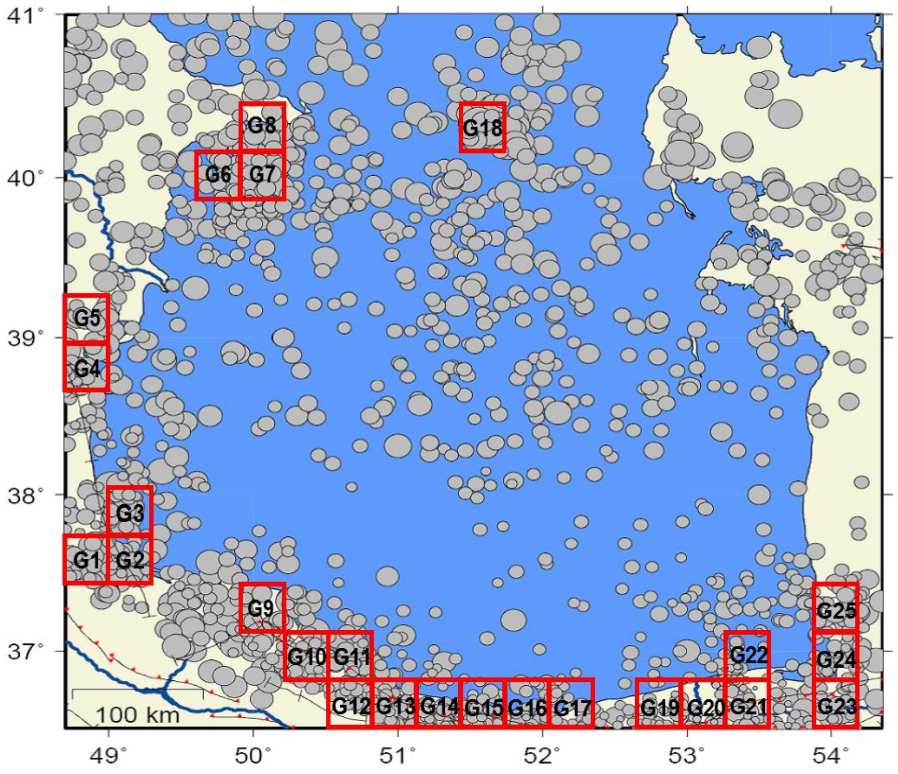

Figure 9: Number of networks in the first series of overlapping grid

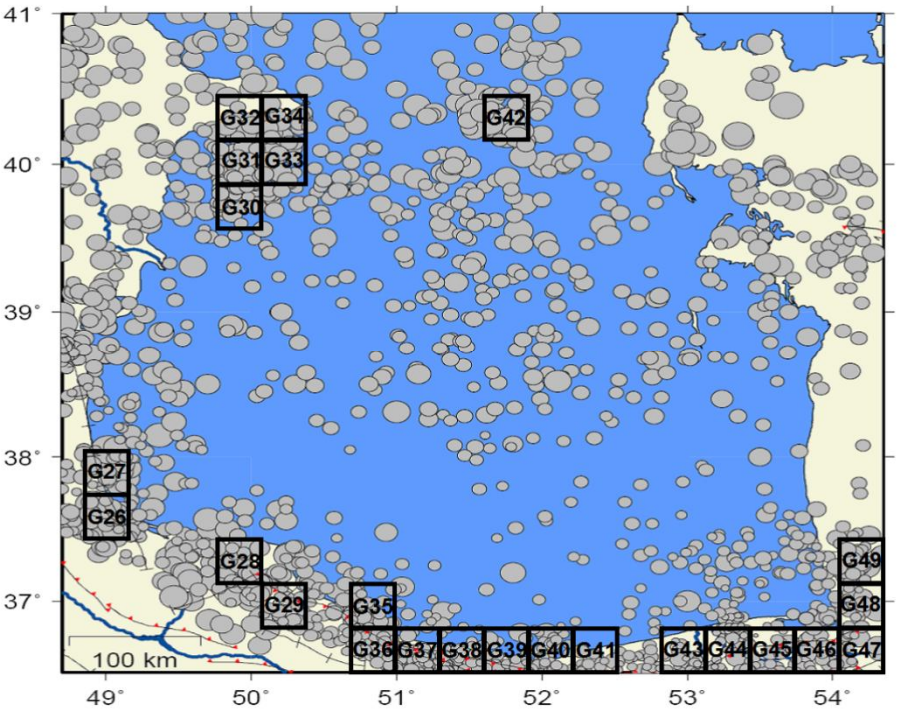

Figure 10: Number of networks in the second series of overlapping grid

After doing the calculations and obtain fractal dimension D (the correlation integral method) for each network (Table 3), the fractal dimension D was varied between 2/180-1/2971.

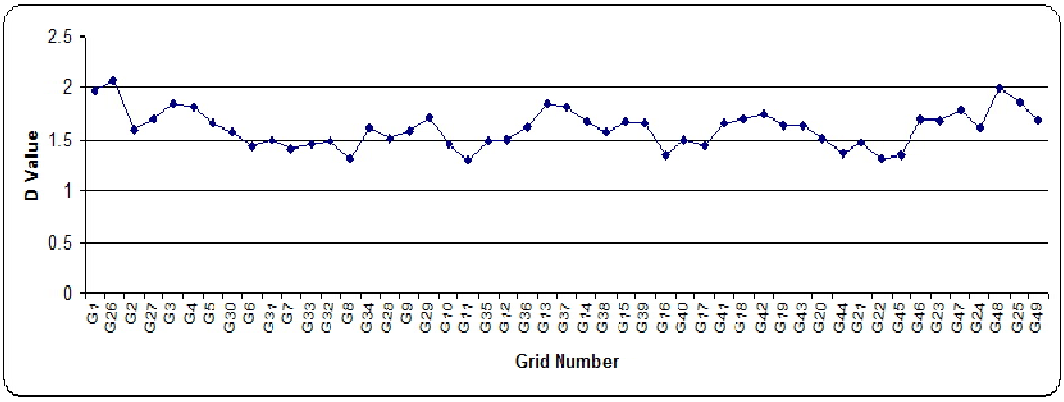

Figure 11: curve D ratio changes in different network

Table 3: correlation integral method for calculating the fractal dimension D network

Grid Number	lonmin	lonmax	Latmin	latmax	D Value	Number of Data in each grid
G1	48.7	49	37.4	37.7	1.9733	28
G2	48.7	49	38.6	38.9	1.6016	28
G3	48.7	49	38.9	39.2	1.8485	21
G4	49	49.3	37.4	37.7	1.8222	21
G5	49	49.3	37.7	38	1.6512	24
G6	49.6	49.9	39.8	40.1	1.4423	28
G7	49.9		37.1	37.4	1.4128	24
G8	49.9	50.2	39.8	40.1	1.3127	40
G9	49.9	50.2	40.1	40.4	1.5897	22
G10	50.2	50.5	36.8	37.1	1.4495	24
G11	50.5	50.8	36.5	36.8	1.2971	22
G12	50.5	50.8	36.8	37.1	1.5036	30
G13	50.8	51.1	36.5	36.8	1.8395	53
G14	51.1	51.4	36.5	36.8	1.6787	50
G15	51.4	51.7	36.5	36.8	1.6742	47
G16	51.4	51.7	40.1	40.4	1.359	27
G17	51.7	52	36.5	36.8	1.438	51
G18	52	52.3	36.5	36.8	1.707	37
G19	52.6	52.9	36.5	36.8	1.6484	23
G20	52.9	53.2	36.5	36.8	1.5119	23
G21	53.2	53.5	36.5	36.8	1.4668	31
G22	53.2	53.5	36.8	37.1	1.3064	23
G23	53.8	54.1	36.5	36.8	1.6907	22
G24	53.8	54.1	36.8	37.1	1.6072	22
G25	53.8	54.1	37.1	37.4	1.8584	21
G26	48.85	49.15	37.4	37.7	2.081	24
G27	48.85	49.15	37.7	38	1.7052	23
G28	49.75	50.05	37.1	37.4	1.5183	26
G29	49.75	50.05	39.5	39.8	1.7202	21
G30	49.75	50.05	39.8	40.1	1.5667	52
G31	49.75	50.05	40.1	40.4	1.5012	20
G32	50.05	50.35	36.8	37.1	1.4808	23
G33	50.05	50.35	39.8	40.1	1.4549	20
G34	50.05	50.35	40.1	40.4	1.6098	20
G35	50.65	50.95	36.5	36.8	1.4864	40
G36	50.65	50.95	36.8	37.1	1.6322	31
G37	50.95	51.25	36.5	36.8	1.8152	48
G38	51.25	51.55	36.5	36.8	1.5663	57
G39	51.55	51.85	36.5	36.8	1.6603	45
G40	51.55	51.85	40.1	40.4	1.4974	36
G41	51.85	52.15	36.5	36.8	1.6602	53
G42	52.15	52.45	36.5	36.8	1.7372	20
G43	52.75	53.05	36.5	36.8	1.6465	28
G44	53.05	53.35	36.5	36.8	1.3714	21
G45	53.35	53.65	36.5	36.8	1.3589	28
G46	53.65	53.95	36.5	36.8	1.706	20
G47	53.95	54.25	36.5	36.8	1.7847	21
G48	53.95	54.25	36.8	37.1	1.999	27
G49	53.95	54.25	37.1	37.4	1.6915	34

3. CONCLUSION

As specified in figure (11), the form (11) is, the fractal dimension is a generally high, It was the case that as the fractal dimension for earthquake induction is generally less than one. But the remarkable thing is that the fractal dimension obtained in networks G6, G7, G8 and G10, G11 and G16, G17 and G21, G22 series overlaps the first and networks, G31, G32, G33 and G35, and G40 and G44, G45 series of overlapping second the rest of the network is less**.** Network location G6, G7, G8 and G31, G32, G33 precisely place the quake a magnitude 5.8 and its aftershocks are consistent As the form (5) is significantly associated with the earthquake and aftershocks rocked her well Mogi model for type 2 induced earthquakes follow, And as shown in Figure (6) the decay rate of aftershocks to this earthquake (h = 1.052) in good agreement with the decay rate of aftershocks for induced earthquakes. Due to the good adaptation patterns and most networks in the region since the fractal dimension is 1.5, Lower coefficient D in these networks can result in the induction of Caspian pressure on pore pressure distribution in the lower layers of skin or shell is Lake Because the studies and Harish Rajendran (2000), their model is based on the distribution of water in the porous layer induced earthquakes in the region to justify Koyna - Varna offered**.** High permeability and the fluid in the fault and surrounding areas can be effective in reducing the stress, since relatively low compared to other surrounding areas have seen D coefficients. Coefficient D can also reduce the effect of pore water pressure in the lake area; the pore water pressure caused the redistribution of stresses in the lower layers of the crust. Thus it can be said that the observations made in the Caspian Sea with an M = 5.8 in 2000/11/25 earthquakes are induction type. It is thought that the load induced changes in Caspian stress distribution and heterogeneity of the mantle beneath the crust of the occurrence of these earthquakes have been associated with a M=5.8.

REFERENCES

1. Aviles, C. A., Scholz, C. H., and Boatwright, J., 1987, Fractal analysis applied to characteristic segments of the San Andreas fault, J. Geophys. Res., 92, 331-341.

2. Bhattacharya, P. M., Majumder, R. K., and Kayal, J. R., 2002, Fractal dimension and b-value mapping in northeast India, Curr. Sci., 82, 1486-1491.

3. Chandrani, S., Bhattacharya P. M., and Chadha R., K., 2008, Seismicity in the Koyna-Warna Reservoir Site in Western India: Fractal and b- Value Mapping, B. Seismol. Soc. Am., 98, 476-482.

4. DeRubeis, V., Dimitriu, P., Papadimitriou, E. and Tosi, R., 1993, Recurrent patterns in the spatial behaviour of Italian seismicity revealed by the fractal approach, Geophys. Res. Lett., 20, 1911-1914.

5. Engdahl, E. R., Jackson, J. A., Myers, S. C., Bergman, E. A., and Priestley, K., 2006, Relocation and assessment of seismicity in the Iran region, Geophys. J. Int., 167, 761-779.

6. Grassberger, P., and Procaccia, I., 1983, Characterization of strange attractors, Phys. Rev. Lett., 50, 346-349.

7. Gupta, H., K., Rastogi, B., K., and Hari N., 1972, Common features of the reservoir associated seismic activities, B. Seismol. Soc. Am., 62, 481-492.

8. Gutenberg, B., and Richter, C. F., 1949, Seismicity of the Earth, Princeton Univ. Press Cambridge UK. Henderson, J. R., Barton, D. J., and Foulger, G.

9. R., 1999, Fractal clustering of induced seismicity in the Geysers geothermal area, California, Geophys. J. Int., 139, 317-324.

10. Hirata, T., 1989, A correlation between the bvalue and the fractal dimension of earthquakes, J. Geophys. Res., 94, 7507-7514.

11. Kagan, Y. Y., 2007, Earthquake spatial distribution: the correlation dimension, Geophys. J. Int., 168, 1175-1194.

12. Kagan, Y., Y., and Knopoff, L., 1980, Spatial distribution of earthquakes: the two-point correlation function, Geophys. J. R. Astr. Soc., 62, 303-320.

13. King, G., 1983, The accommodation of large strains in the upper lithosphere of the earth and other solids by self-similar fault systems: The geometrical origin of b-value, Pure appl. Geophys., 121, 761-815.

14. Lapenna, V., Macchiato, M., and Telesca, L., 1998, 1/ f β fluctuations and selfsimilarity in earthquake dynamics-observational evidences in southern Italy, Phys. Earth planet. Inter., 106, 115-127.

15. Legrand, D., 2002, Fractal dimensions of small, intermediate, and large earthquakes, B. Seismol. Soc. Am., 92, 3318-3320.

16. Legrand, D., Cistemas, A., and Dorbath, L., 1996, Mulifractal analysis of the 1992. Erzincan aftershock sequence, Geophys. Res. Lett., Phys. Lett. 23, 933-936.

17. Mandal, P. and Rastogi, B. K., 2005, Selforganized fractal seismicity and b value of aftershocks of the 2001 Bhuj earthquake in Kutch (India), Pure appl. Geophys., 162, 53- 72.

18. Mandelbrot, B. B., 1982, The Fractal Geometry of Nature, Freeman, San Francisco, 468 pp.

19. Mogi, K., 1962, Magnitude-frequency relation for elastic shocks accompanying fractures of various materials and some related problems in earthquakes, Bull. Earthquake Res. Inst. Tokyo Univ., 40, 831-853.

20. Okubo, P. G., and Aki, K., 1987, Fractal geometry in the San Andreas fault system, J.Geophys. Res., 92, 345-355.

21. Oncel, A. O., Main, I., Alptekin, O., and Cowie, P., 1996. Temporal variations in the fractal properties of seismicity in the north Anatolian fault zone between 31◦E and 41◦E, Pure appl. Geophys., 147, 147-159.

22. Pickering, G., Bull, J. M., and Sanderson, D. J., 1995, Sampling power-law distributions, Tectonophysics, 248, 1-20.

23. Rajendran, K., and Harish, C. M., 2000, Mechanism of triggered seismicity at Koyna:an evaluation based on relocated earthquakes, Curr. Sci 79, 358-363.

24. Shimazaki, K., and Nagahama, H., 1995, Do earthquakes break out irregularly? Collective and individual characters of earthquakes, Kagaku (Science), 65, 241-256.

25. Simpson, D. W., Leith, W. S., and Scholz, C. H., 1988, Two types of reservoir-induced seismicity, B. Seismol. Soc. Am., 78, 2025- 2040.

26. Simpson, D. W., 1976, Seismicity changes associated with reservoir impounding, Eng. Geol., 10, 371-85. Smith, W. D., 1981, The b-value as an earthquake precursor, Nature, 289, 136-139.

27. Tosi, P. 1998, Seismogenic structure behavior revealed by spatial clustering of seismicity in the Umbria- Marche Region (central Italy), Ann. Geophys., 41, 215-224.

28. Turcotte, D. L., 1986, A fractal model for crustal deformation, Tectonophysics, 132, 261-269.

29. Utsu, T., 1965, A method for determining the value of b in the formula logN = a-bM,

30. showing the frequency-magnitude relation for earthquakes, Geophy. Bull., Hokkaido uni., 13, 99-103.

31. Volant, P., and Grasso, J. R., 1994, The finite extension of fractal geometry and power-law distribution of shallow earthquakes–a geomechanical effect, J. geophys. Res., 99, 21879-21889.

32. Wang, J. H., 1991, A note on the correlation between b-value and fractal dimension from synthetic seismicity, Terrest., Atmos. Oceanic Sci., 2, 317-329.

33. Wyss, M., Sammis, C. G., Nadeau, R. M., and Wiemer, S., 2004, Fractal dimension and bvalue on creeping and locked patches of the San-Andreas fault near Parkfield, California, B. Seismol. Soc. Am., 94, 410-421.

34. Wyss, M., 1973, Towards a physical understanding of the earthquake frequency distribution, Geophys. J. R. Astr. Soc., 31, 341-359.

35. Wyss, M., and Stefansson, R., 2006, Nucleation points of recent mainshocks in southern Iceland mapped by b-values, B. Seismol. Soc. Am., 96, 599-608.